Ab Initio Study of Radical Reactions: Role of Coupled Internal Rotations on the Reaction Kinetics (III)

V. Van Speybroeck,* D. Van Neck, and M. Waroquier

Laboratory of Theoretical Physics, Universiteit Gent, Proeftuinstraat 86, B-9000 Gent, Belgium

Received: March 26, 2002

The reaction kinetics of two radical reactions that are important for coke formation during the thermal cracking of hydrocarbons is studied by transition-state theory. It is investigated how coupled internal rotations influence the partition functions of molecules with several torsional motions and the reaction kinetics involving such molecules. This is done by applying a general scheme, which is able to treat various rotating tops without restrictions on the symmetry of the rotating parts.

1. Introduction

In this paper, the attention is focused on the role of coupled internal rotations on the kinetics of radical reactions. The chemical reactions under study are of importance within the thermal cracking of hydrocarbons, which is one of the main processes for the production of light olefins such as ethene. During the thermal cracking, a coke layer is formed on the inner walls of the reactor, which exhibits a negative influence on the efficiency of the reactor unit. The process of coke fomation is complex and consists of thousands of elementary radical reactions. These can be classified in a limited number of classes such as hydrogen abstraction, addition, and cyclization reactions. To unravel the complex mechanism of coke formation, some prototype reactions are searched that are representative for the kinetics of each class. In two previous papers of the authors,[1,2] the kinetics of two basic reactions—the addition reaction of ethene toward the butylbenzene radical and the subsequent cyclization reaction (Figure 1)—was studied by means of transition-state theory.[3] The basic quantities for the reaction rate expression are the energy difference between the transition state and the ground state at the absolute zero and the partition functions. All of these quantities are determined by ab initio density functional theory calculations at the B3LYP/6-311G** level of theory.[4−6] One of the main difficulties for the molecules under study is the presence of one or more hindered internal rotors. In refs 1 and 2, we found that low vibrational modes that correspond to internal rotations should be correctly described to obtain accurate predictions for the preexponential factor.

In principle, all internal rotations are coupled with each other and with the overall rotation of the molecule. This makes an exact treatment rather cumbersome. In refs 1 and 2, we treated all internal rotations as uncoupled. By this approach, one goes beyond the harmonic oscillator (HO) approximation because more conformers are taken into account, that is, all conformers that can be reached by following a one-dimensional path on the potential energy surface. This is illustrated for the butylbenzene radical; Figure 2 shows the two-dimensional rotational energy surface in terms of the internal rotations characterized by variations of the torsional angles ϕ_2 (propylene rotation) and ϕ_3 (ethylene rotation). In the uncoupled internal rotor approach, the conformers BB1, BB2, and BB3 are taken into account correctly, while the exact location of the minima corresponding to BB4 and BB5 are not correctly described in the uncoupled scheme. As also stated in ref 7, the location of the maxima on the coupled and uncoupled surface can also be significantly different. The attention is focused on the mentioned specific torsional motions because they are the most significant to reach the various conformers of the butylbenzene radical. Despite the

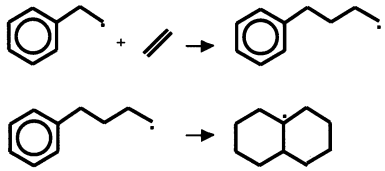

Figure 1. Addition of the ethylbenzene radical to ethene and cyclization of the butylbenzene radical.

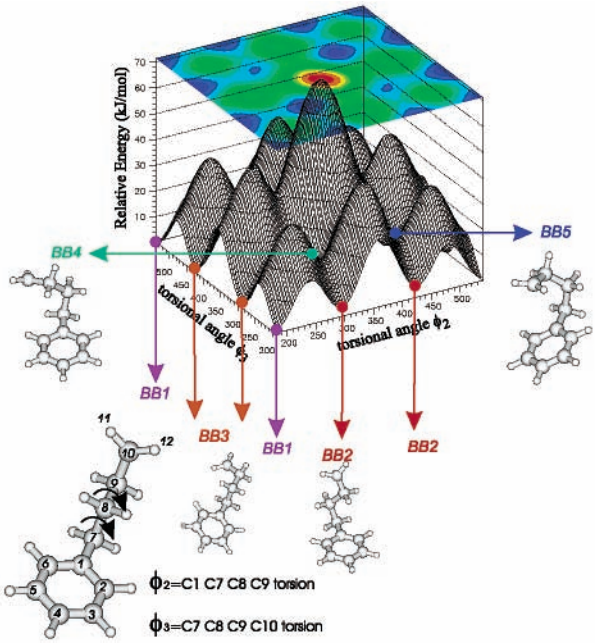

Figure 2. Two-dimensional potential energy surface, $V_{BB}(\phi_2,\phi_3)$, for the butylbenzene radical and the stable conformers on the surface.

* To whom correspondence should be addressed. Fax: 32 (0)9 264 65 60. E-mail: veronique.vanspeybroeck@rug.ac.be.

10.1021/jp025836y CCC: $22.00
Published on Web 08/29/2002

topographical similarity of both surfaces, one can question the impact of the observed discrepancies on the kinetics of the reactions under study, which was still an open question in refs 1 and 2.

Since the pioneering work of Pitzer,[8] which showed that torsions about single bonds are not freely rotating, there have appeared many books and reviews on hindered rotations.[9,10] The theory of hindered rotors is well-known but has been too cumbersome for many applications because it explodes in complexity once coupling is taken into consideration making extended numerical applications almost unfeasible. Many approximative schemes have been presented. The most common approximation is to treat rotating tops symmetrically. For this case, Pitzer presented tables for various thermodynamic functions, but they are also inconvenient for use in computer programs. Also some functions were presented that can estimate thermodynamic functions without having to start from first principles for each application.[11,12] The problem of coupled internal rotations was addressed in few studies to determine far-infrared torsional spectra of molecules.[13,14] Rotor−rotor coupling was also described in a paper of East and Radom to determine third-law entropies up to 1 J mol^{-1} K^{-1}.[7] However, up to now, only schemes that treat coupled symmetrical tops were presented. Moreover, the potential energy surface is systematically described by limited Fourier series, of which the expansion coefficients are fitted to conformation energies obtained by ab initio calculations. In this paper, we go beyond this approach, by presenting an algorithm that is able to treat coupled internal rotations of asymmetric rotating tops with no limit upon the number of rotating tops. The potential energy is constructed in a fully ab initio way with no limits upon the symmetry. We apply the scheme to the two reactions of interest in this paper, but it should be stressed that the algorithm is of general applicability.

2. Theoretical Procedures

All ab initio calculations were carried out with the Gaussian 98 software package.[15] All stable conformers of reactants, products, and transition states are taken from refs 1 and 2. These were calulated at the DFT/6-311G** level of theory.[4−6] According to several references in the literature[16] on similar reactions, this level of theory gives reliable predictions of geometries and frequencies for a realistic computational time. For more details about the specific computational procedures, we refer to refs 1 and 2.

For an exact treatment of internal rotations, one must analyze the low vibrational spectrum of the molecules at hand and identify the motions that correspond with internal rotations.[1,2] For two rotating tops, one can obtain the following torsional Hamiltonian, starting from the general expression for the classical kinetic energy as given in the work of Pitzer:[8]

$$H_T = \frac{1}{2}AJ_2^2 + \frac{1}{2}BJ_3^2 + CJ_2J_3 + V(\phi_2,\phi_3) \qquad (1)$$

where J_2 and J_3 are the internal angular momenta defined by $J_{2(3)} = (\partial T/(\partial \omega_{2(3)})$ with ω_2 and ω_3 being the angular velocities about the rotation axes of the two internal rotations and T being the kinetic energy. $V(\phi_2,\phi_3)$ represents the two-dimensional rotational energy potential. For the specific reactions under study, the two-dimensional rotational potential is constructed for the butylbenzene radical by building a two-dimensional grid ranging from 180° to 540° in both dimensions. For each point, the potential is calculated at the UHF/6-31G* level[17] by optimizing all variables with constrained ϕ_2 and ϕ_3 angles. The same procedure is applied to the transition state for the addition reaction. The coefficients A, B, and C in eq 1 are functions of the two torsional angles; the exact expression can be found in refs 18 and 19.

The partition function corresponding to the two coupled internal rotations can be determined either quantum mechanically or, in the high-temperature limit, classically. We adopt both schemes to test the influence of the temperature range on the thermodynamic quantities. At high temperatures, the canonical partition function has significant contributions from a large number of quantum states. In this limit, the summation over states can be approximated as an integral over phase space:

$$q_{\mathrm{eth,prop}}^{\mathrm{class}} = \frac{1}{(2\pi)^2}\int \mathrm{d}J_2\,\mathrm{d}J_3\,\mathrm{d}\phi_2\,\mathrm{d}\phi_3\,\mathrm{e}^{-H_T/(k_BT)} = \frac{k_BT}{2\pi}\int \mathrm{d}\phi_2\,\mathrm{d}\phi_3\frac{\mathrm{e}^{-V(\phi_2,\phi_3)/(k_BT)}}{\sqrt{AB-C^2}} \qquad (2)$$

In the low-temperature limit, the partition function must be determined quantum mechanically by determining all energy eigenvalues of the two-dimensional differential equation:

$$\hat{H}_T\psi_i(\phi_2,\phi_3) = \epsilon_i\psi_i(\phi_2,\phi_3) \qquad (3)$$

$\hat{H}_T$ is obtained by regarding the angular momenta J_2 and J_3 in eq 1 as quantum-mechanical operators. The partition function can then be obtained by a summation over all energy states up to convergence:

$$q_{\mathrm{eth,prop}}^{\mathrm{qm}} = \frac{1}{\sigma_{\mathrm{int}}}\sum_i g_i\,\mathrm{e}^{-\epsilon_i/(k_BT)} \qquad (4)$$

where g_i is the degeneracy of the rotational energy level ϵ_i and σ_{int} is the internal symmetry number of the coupled internal rotors. The symmetry number has to be introduced to prevent overcounting of the number of unique minima. In our case, σ_{int} equals 1 because the symmetry number for both rotations is 1.

We have solved the resulting coupled differential equation by a new numerical algorithm based on perturbation theory of the partition function. The details are outlined in ref 20. We first determine the variationally best product wave function $\psi_i(\phi_2,\phi_3) = f(\phi_2)g(\phi_3)$, which minimizes the expectation value of $\hat{H}_T$. This results in self-consistent fields, $\hat{H}_0 = \hat{h}_{02}(\phi_2) + \hat{h}_{03}(\phi_3)$, which already contain the averaged effects of rotational coupling. Next, we use the basis of product eigenstates of $\hat{H}_0$ to evaluate the partition function up to second order in $\hat{\Delta} = \hat{H}_T - \hat{H}_0$. We find that this method, which avoids the large dimensionality of the full coupled rotor space, leads to numerically stable results.

3. Results and Discussion

Partition Functions Determined Quantum Mechanically and Classically. Figure 3a shows the partition function in terms of temperature associated with the (uncoupled) ethylene internal rotation in the butylbenzene radical, calculated both quantum mechanically and classically. Figure 3b shows the classical and quantum mechanical partition function of the coupled ethylene and propylene internal rotations in the butylbenzene radical. It is observed that quantum mechanical effects are only important for temperatures up to 150 K. At higher temperatures, the classical approximation becomes almost exact.

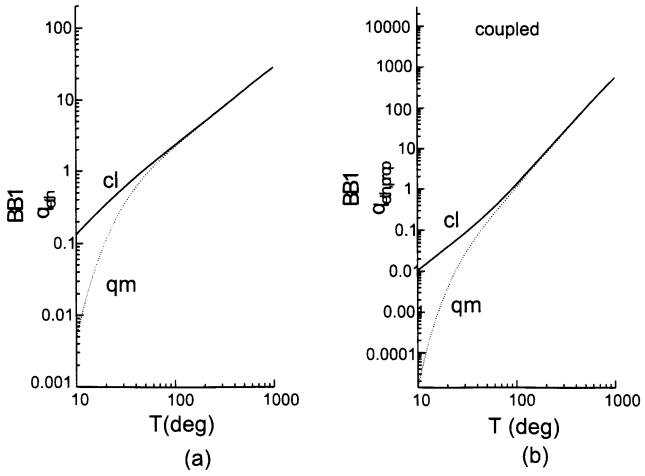

Figure 3. Partition function for (a) the ethylene internal rotation in the butylbenzene radical and (b) the coupled ethylene and propylene internal rotations in the butylbenzene radical, calculated classically (cl) and quantum mechanically (qm).

Influence of Internal Rotations on the Partition Functions. Figure 4a,b shows the partition function associated with the ethylene and propylene internal rotation in the butylbenzene radical (BB1) and the transition state for the addition reaction (TSBB1) in terms of the temperature in various approximative schemes. The partition function obtained by treating the two internal rotations in the harmonic oscillator approximation (vibrational mode) represents the standard in all ab initio packages. The partition function is largely enhanced by replacing the harmonic oscillator model by internal rotations. This is best visualized in Figure 4a,b by the IR/uncoupled B3LYP result, whereby the two internal rotations under study are handled as uncoupled internal rotors with rotational potentials determined at the B3LYP/6-311G** level of theory.

To get an idea about the impact of the level of theory on the partition function, we replace the ethylene and propylene rotational potentials of the previous case by cuts from the two-dimensional potential energy surface at $\phi_2 = 180°$ and $\phi_3 = 180°$, which has been determined at the UHF/6-31G* level. The result is given by IR/uncoupled B3LYP/UHF. The reference geometries and all internal rotations are determined at the B3LYP/6-311G** level, except that the ethylene and propylene rotational potentials are determined at the UHF/6-31G* level. Finally, Figure 4 also includes the partition function obtained in an exact coupling scheme of the ethylene and propylene rotations, thereby using the two-dimensional energy surface in terms of the two torsional angles.

By going from the harmonic oscillator to the uncoupled internal rotor approach, a serious enhancement of the partition functions is noticed. This can be explained by an increase of the density of states in the low-energy spectrum by taking into account a realistic internal rotor potential compared with a harmonic oscillator potential with infinite wells. As a result, more conformers are accessible in the internal rotor approach, leading to an enhancement of the molecular partition function. The increase in the case of transition state for addition (TSBB1) is more pronounced than that for the butylbenzene radical. This effect can be traced back to the special nature of the ethylene internal rotation in the transition state, which corresponds to the rotation of the approaching ethene around the forming C−C bond. This particular internal mode is a transitional mode, which arises from the loss of one external rotation of ethene when brought together with the ethylbenzene radical. The internal rotor potential predicts that ethene will preferably attack the ethylbenzene radical in the gauche conformation.

It should be stressed that the partition functions are very sensitive to any change of the geometry and the level of theory. Even a small reduction of the rotational potential barriers may lead to a serious change of the partition function. In Figure 5, the propylene and ethylene internal rotations are described at two different levels of theory (the potentials are determined, respectively, at $\phi_2 = 180°$ and $\phi_3 = 180°$). In the case of the butylbenzene radical, the B3LYP/6-311G** prediction slightly underestimates the potential barriers with respect to UHF/6-31G*, causing a small shift of the bound rotational levels to lower energies. This immediately manifests in a substantial increase of the corresponding partition functions. For the transition state TSBB1, the potential barriers are almost similar, but the propylene rotational shape slightly changes with the level of theory. Anyway, in this case, we observe practically no deviation and the partition functions are coinciding with each other. These results agree with some conclusions made by Heuts et al.[21] One should be very careful in drawing general conclu-

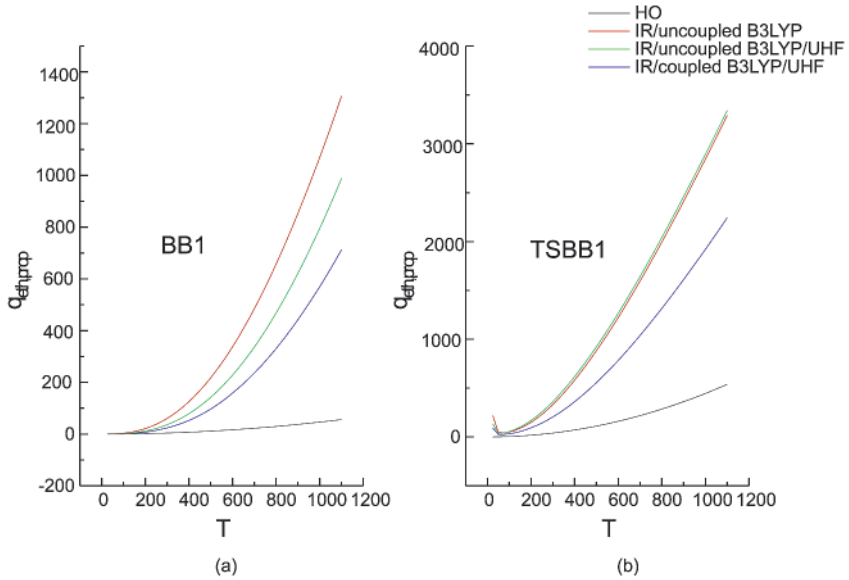

Figure 4. Partition function of the ethylene and propylene internal rotations in (a) the butylbenzene radical and (b) the transition state for the addition reaction in terms of temperature in various approximative schemes.

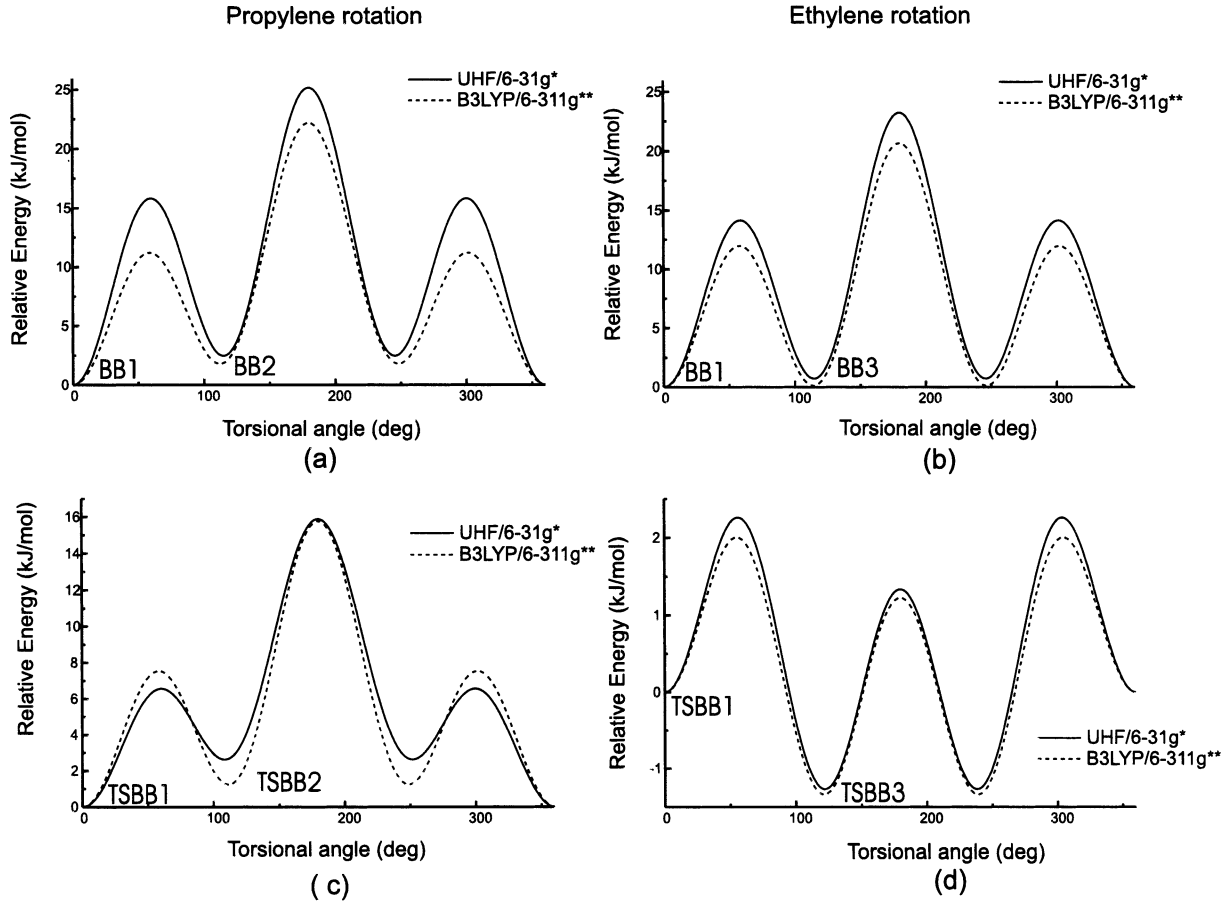

Figure 5. The rotational potentials at various levels of theory for the ethylene and propylene motions in the butylbenzene radical (parts a and b) and the transition state for the addition reaction (parts c and d).

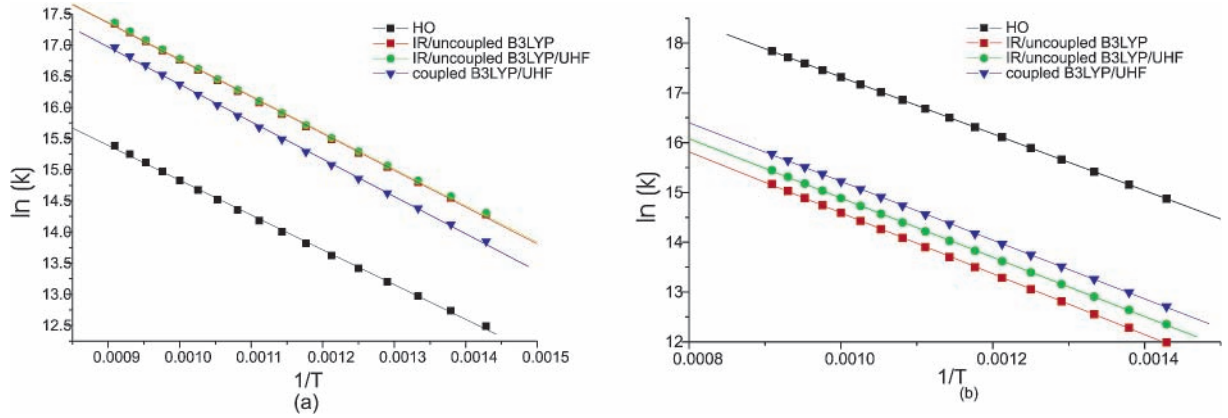

Figure 6. Arrhenius plot for (a) the addition reaction and (b) the cyclization reaction in the temperature range from 700 to 1100 K.

sions, but it appears that relatively low levels of theory, which are less time-consuming, are sufficient for the evaluation of the partition function within 25%. Finally, application of the exact coupling scheme of the two primary internal rotations in the BB1 and TSBB1 conformers leads to a decrease of the partition function compared with the uncoupled internal rotor approach and seems to moderate the effect of treating internal rotations. However, the values are still larger than those in the HO approximation. The origin can be traced back to the specific nature of the coupled rotational potential compared with the uncoupled two-dimensional potential, which can be constructed by taking the sum $V(\phi_2) + V(\phi_3)$. The true two-dimensional rotational energy surface for the butylbenzene radical shows a large central bump, which shifts up the energy levels in the low-energy spectrum, leading to a decrease of the partition function. Physically, it means that it is more difficult to "walk" through the "coupled potential energy surface" than through the "uncoupled surface".

Influence of Internal Rotations on the Kinetic Parameters. By calculating the partition functions at various temperatures, one can construct an Arrhenius plot and determine the pre-exponential factor and activation energy of the reactions. The rate equation for a bimolecular reaction $A + B \rightarrow C$ obeys

$$k(T) = \frac{k_B T}{h} \frac{q_{\ddagger}/V}{(q_A/V)(q_B/V)} e^{-\Delta E_0/(k_B T)} \qquad (5)$$

and is expressed in units of $dm^3\ s^{-1}$ (h is the Planck constant),

TABLE 1: Kinetic Parameters for the Addition and Cyclization Reactions[a]

		addition reaction		cyclization reaction	
		forward	reverse	forward	reverse
ΔE_0		31.02	109.28	51.79	75.93
E_a	HO-B3LYP/6-311G**	46.44	115.98	47.44	82.27
	IR-uncoupled-B3LYP/6-311G**	49.12	115.97	50.89	82.27
	IR-uncoupled-B3LYP/6-311G**//UHF/6-31G*	48.91	114.38	49.51	82.27
	IR-uncoupled-B3LYP/6-311G**//UHF/6-31G*	49.87	114.88	49.04	82.27
A	HO-B3LYP/6-311G**	7.27×10^8	1.18×10^{14}	1.00×10^{10}	6.14×10^{13}
	IR-uncoupled-B3LYP/6-311G**	6.91×10^9	8.89×10^{13}	9.90×10^8	6.14×10^{13}
	IR-uncoupled-B3LYP/6-311G**//UHF/6-31G*	6.86×10^9	1.00×10^{14}	1.13×10^9	6.14×10^{13}
	IR-coupled-B3LYP/6-311G**//UHF/6-31G*	5.11×10^9	9.87×10^{13}	1.49×10^9	6.14×10^{13}

[a] ΔE_0 represents the reaction barrier at 0 K and is defined as the molecular binding energy difference between transition state and reactants in the forward reaction and between transition state and product in the reverse reaction (including zero-point energies). The kinetic parameters are given by the activation energy and the preexponential factor and determined by various schemes: HO approximation, the uncoupled internal rotor approximation with use of B3LYP/6-311G** rotational potentials, the uncoupled internal rotor approximation with use of UHF/6-31G* rotational potentials for the ethylene and propylene motion and B3LYP/6-311G** potentials for all other internal rotations, and the coupled internal rotor approximation with same level of theory of the previous case. All energies are in kJ/mol. The preexponential factors are expressed in units dm^3/(mol s) for the forward addition reaction and 1/s for all other reactions.

while for a unimolecular reaction, $A \rightarrow B$, the rate constant is given by

$$k(T) = \frac{k_B T}{h} \frac{q_\ddagger / V}{q_A / V} e^{-\Delta E_0/(k_B T)} \qquad (6)$$

and is expressed in units of s^{-1}.

In a typical cracking unit, the temperature varies from 700 to 1100 K, in terms of the length of the reactor. The kinetic parameters are determined by fitting in the appropriate temperature range. The resulting Arrhenius plots are shown in Figure 6. Table 1 gives an overview of the theoretically predicted kinetic parameters of the reactions under study obtained in the various approximation schemes. ΔE_0 represents the reaction barrier at 0 K, defined as the energy difference between the transition state and reactants. The activation energies are determined by the slope of the Arrhenius plots (see Figure 6) and are very sensitive to the temperature region in which the Arrhenius parameters are fitted. In the forward addition and cyclization reaction, the activation energies increase by a few kJ/mol when handling internal rotations instead of a treatment of these modes in the harmonic oscillator approach. Preexponential factors turn out to be largely affected. We notice a factor of 10 in the addition reaction, but it should be stressed that in an exact coupling scheme the enhancement factor is mildly reduced. It is an overall conclusion that the uncoupled hindered rotor approximation overestimates the effects generated by the treatment of internal rotations. The coupled scheme moderates these effects, and this is due to the specific nature of the true two-dimensional rotational energy surface. An extra central bump appears (Figure 2) both for the transition state TSBB1 of the addition reaction and for the butylbenzene radical BB1, which makes it more difficult to proceed from one conformer to another in the coupled surface. In the reverse addition reaction, the influence of internal rotors turns out to be small, which is a direct result from canceling effects of the enhanced IR partition functions in the numerator and denominator of the rate equation. The reverse cyclization reaction obviously exhibits no influence of internal rotations because of the complete absence of any internal rotor in reactant and activated complex.

4. Conclusions

In this paper, we studied the influence of the coupling of two internal rotations on the kinetics of two radical reactions that are of importance for the formation of cokes during thermal cracking of hydrocarbons. The specific reactions were already extensively handled in two previous papers of the authors at the DFT/B3LYP/6-311G** level and by treating all internal rotations in an exact but uncoupled way.[1,2] For the specific reactions under study, we found that coupling of internal rotations has a minor influence on the kinetics compared with the corrections already taken up in an uncoupled scheme. It appears that the uncoupled scheme overestimates the changes to the preexponential factors but that it gives an upper limit to what internal rotations are responsible for. The scheme as applied gives a theoretical foundation for an exact treatment of coupled internal rotations. However, to draw more general conclusions on the influence the coupled scheme on the kinetics, a larger set of reactions should be studied for which also accurate experimental data are available. This work is in progress.

Acknowledgment. This work is supported by the Fund for Scientific Research−Flanders (FWO) and the Research Board of Ghent University.

References and Notes

(1) Van Speybroeck, V.; Van Neck, D.; Waroquier, M.; Wauters, S.; Saeys, M.; Marin, G. B. *J. Phys. Chem. A* **2000**, *104* (46), 10939−10950.

(2) Van Speybroeck, V.; Borremans, Y.; Van Neck, D.; Waroquier, M.; Wauters, S.; Saeys, M.; Marin, G. B. *J. Phys. Chem. A* **2001**, *105* (32), 7713−7723.

(3) For reviews, see, for example: (a) Pechukas, P. In *Dynamics of Molecular Collisions, Part B*; Miller, W. H., Ed.; Plenum Press: New York, 1976. (b) Laidler, K. J.; King, M. C. *J. Phys. Chem.* **1983**, *87*, 2657. (c) Truhlar, D. G.; Hase, W. L.; Hynes, J. T. *J. Phys. Chem.* **1983**, *87*, 2664.

(4) Parr, R. G.; Yang, W. *Density-Functional Theory of Atoms and Molecules*; Oxford University Press: New York, 1989.

(5) Becke, A. D. *J. Chem. Phys.* **1993**, *98*, 5648.

(6) Krishnan, R.; Binkley, J. S.; Seeger, R.; Pople, J. A. *J. Chem. Phys.* **1980**, *72*, 650.

(7) East, A. L. L.; Radom, L. *J. Chem. Phys.*, **1997**, *106* (16), 6655.

(8) (a) Pitzer, K. S. *J. Chem. Phys.* **1937**, *5*, 469. (b) Pitzer, K. S.; Gwinn, W. D. *J. Chem. Phys.* **1942**, *10*, 428.

(9) (a) Mizushima, S. *Structure of Molecules and Internal Rotation*; Academic Press: New York, 1954. (b) Orville-Thomas, W. J. *Internal Rotation in Molecules*; Wiley: London, 1974. (c) Lister, D. G.; MacDonald, J. N.; Owen, N. L. *Internal Rotation and Inversion*; Academic Press: London, 1978.

(10) (a) Wilson, E. B., Jr. *Adv. Chem. Phys.* **1959**, *2*, 367. (b) Dale, J. *Tetrahedron* **1966**, *22*, 3373. (c) Lowe, J. P. *Prog. Phys. Org. Chem.* **1968**, *6*, 1. (d) Förster, H.; Vögtle, F. *Angew. Chem.* **1977**, *16*, 429. (e) Long, D. A. *J. Mol. Struct.* **1985**, *126*, 9. (f) Berg, U.; Sandström, J. *Adv. Phys. Org. Chem.* **1989**, *25*, 1.

(11) Truhlar, D. G. *J. Comput. Chem.* **1991**, *12*, 266.

(12) McClurg, R. B.; Flagan, R. C. *J. Chem. Phys.* **1997**, *106* (16), 6675.

(13) East, A. L. L. *J. Chem. Phys.* **1997**, *107* (10), 3914.

(14) Wesenberg, G.; Weinhold, F. *Int. J. Quantum Chem.* **1982**, *21*, 487−509. Senent, M. L.; Smeyers, Y. G. *J. Chem. Phys.* **1996**, *105* (7),

2789. Senent, M. L.; Smeyers, Y. G.; Moule, D. C. *J. Phys. Chem. A* **1998**, *102*, 6730−6736. Smeyers, Y. G.; Senent, M. L.; Botella, V.; Moule, D. C. *J. Chem. Phys.* **1993**, *98* (4), 2754. Smeyers, Y. G.; Bellido, M. N. *Int. J. Quantum Chem.* **1981**, *19*, 553−565. Vivier-Bunge, A.; Uc, V. H.; Smeyers, Y. G. *J. Chem. Phys.* **1998**, *109* (6), 2279.

(15) Frisch, M. J.; Trucks, G. W.; Schlegel, H. B.; Scuseria, G. E.; Robb, M. A.; Cheeseman, J. R.; Zakrzewski, V. G.; Montgomery, J. A., Jr.; Stratmann, R. E.; Burant, J. C.; Dapprich, S.; Millam, J. M.; Daniels, A. D.; Kudin, K. N.; Strain, M. C.; Farkas, O.; Tomasi, J.; Barone, V.; Cossi, M.; Cammi, R.; Mennucci, B.; Pomelli, C.; Adamo, C.; Clifford, S.; Ochterski, J.; Petersson, G. A.; Ayala, P. Y.; Cui, Q.; Morokuma, K.; Malick, D. K.; Rabuck, A. D.; Raghavachari, K.; Foresman, J. B.; Cioslowski, J.; Ortiz, J. V.; Stefanov, B. B.; Liu, G.; Liashenko, A.; Piskorz, P.; Komaromi, I.; Gomperts, R.; Martin, R. L.; Fox, D. J.; Keith, T.; Al-Laham, M. A.; Peng, C. Y.; Nanayakkara, A.; Gonzalez, C.; Challacombe, M.; Gill, P. M. W.; Johnson, B. G.; Chen, W.; Wong, M. W.; Andres, J. L.; Head-Gordon, M.; Replogle, E. S.; Pople, J. A. *Gaussian 98*, revision A.7; Gaussian, Inc.: Pittsburgh, PA, 1998.

(16) (a) Wong, M. W.; Radom, L. *J. Phys. Chem. A* **1998**, *102*, 2237−2245. (b) Parker, C. L.; Cooksy, A. L. *J. Phys. Chem. A* **1998**, *102*, 6186−6190. (c) Lynch, B. J.; Fast, P. L.; Harris, M.; Truhlar, D. G. *J. Phys. Chem. A* **2000**, *104*, 4811−4815. (d) Smith, D. M.; Nicolaides, A.; Golding, B. T.; Radom, L. *J. Am. Chem. Soc.* **1998**, *120*, 10223−10233.

(17) (a) Roothaan, C. C. J. *Rev. Mod. Phys.* **1951**, *23*, 69. (b) Pople, J. A.; Nesbet, R. K. *J. Chem. Phys.* **1954**, *22*, 571. (c) McWeeny, R.; Dierksen, G. *J. Chem. Phys.* **1968**, *49*, 4852.

(18) Van Speybroeck, V. Ab initio static and dynamic molecular methods: A useful tool in the study of chemical reactions. Ph.D. Thesis, Ghent University, Ghent, Belgium, 2001.

(19) Van Speybroeck, V.; Van Neck D.; Waroquier, M., manuscript in preparation.

(20) Van Neck, D. et al., manuscript in preparation.

(21) Heuts, J. P. A.; Gilbert, R. G.; Radom, L. *J. Phys. Chem.* **1996**, *100*, 18997−19006. Heuts, J. P. A.; Gilbert, R. G.; Radom, L. *Macromolecules* **1995**, *28*, 8771−8781.